



Geophysical Research Letters

RESEARCH LETTER

10.1002/2017GL075965

Key Points:

- A nonstandard method was employed to provide a scientific measurement on the surface of Mars
- Sedimentary structure matters when determining rock strength
- Strengthwise, the sedimentary rocks at Gale crater are more akin to younger sedimentary rock on Earth

Correspondence to:

G. H. Peters,
ghpeters@jpl.nasa.gov

Citation:

Peters, G. H., Carey, E. M., Anderson, R. C., Abbey, W. J., Kinnett, R., Watkins, J. A., ... Vasavada, A. R., (2018). Uniaxial compressive strengths of rocks drilled at Gale crater, Mars. *Geophysical Research Letters*, 45, 108–116. <https://doi.org/10.1002/2017GL075965>

Received 6 OCT 2017

Accepted 22 DEC 2017

Accepted article online 29 DEC 2017

Published online 15 JAN 2018

Uniaxial Compressive Strengths of Rocks Drilled at Gale Crater, Mars

G. H. Peters¹ , E. M. Carey¹, R. C. Anderson¹, W. J. Abbey¹, R. Kinnett¹, J. A. Watkins², M. Schemel², M. O. Lashore¹, M. D. Chasek³, W. Green¹, L. W. Beegle¹, and A. R. Vasavada¹ 

¹Jet Propulsion Laboratory, California Institute of Technology, Pasadena, CA, USA, ²Division of Geologic and Planetary Sciences, California Institute of Technology, Pasadena, CA, USA, ³Department of Geoscience, Chadron State College, Chadron, NE, USA

Abstract Measuring the physical properties of geological materials is important for understanding geologic history. Yet there has never been an instrument with the purpose of measuring mechanical properties of rocks sent to another planet. The Mars Science Laboratory (MSL) rover employs the Powder Acquisition Drill System (PADS), which provides direct mechanical interaction with Martian outcrops. While the objective of the drill system is not to make scientific measurements, the drill's performance is directly influenced by the mechanical properties of the rocks it drills into. We have developed a methodology that uses the drill to indicate the uniaxial compressive strengths of rocks through comparison with performance of an identically assembled drill system in terrestrial samples of comparable sedimentary class. During this investigation, we utilize engineering data collected on Mars to calculate the percussive energy needed to maintain a prescribed rate of penetration and correlate that to rock strength.

Plain Language Summary The one tool that personifies the field geologist is a rock hammer. The field geologist will use his/her hammer to expose fresh rock surfaces allowing examination of unweathered rock. He/she will also use it to determine qualitative rock strengths in the field. While Curiosity does not carry a traditional rock hammer, it does have a drill system. The ability to fail rock with a hammering mechanism and the ability to use the performance data from the drill system presented the authors with an innovative concept. The drill could be used as an instrument to indicate the strength of rocks, except that the drill's measurement is better. Where the field geologist has only his/her tactile senses, Curiosity is instrumented with sensors that measure rates of penetration, percussive energy, and weight on bit allowing a quantifiable measurement of rock strength. The article describes the methodologies that allow the drill system aboard the Mars Science Laboratory rover to also serve as a scientific instrument and reports the compressive strength of the rocks drilled on Mars using these methods.

1. Introduction

The Mars Science Laboratory (MSL) rover, Curiosity, arrived at Bradbury Landing in Gale crater on 6 August 2012, with a payload designed to identify and evaluate the geologic, environmental, and habitability histories of Gale crater (Grotzinger, 2014). To help accomplish this, Curiosity was equipped with a rotary-percussive drill system (Anderson et al., 2012) that, to date, has collected and processed 15 samples from sedimentary rocks of the Yellowknife Bay, Kimberley, Murray, and Stimson formations (Arvidson, 2016).

The MSL Powder Acquisition Drill System (PADS) is located on the turret assembly at the end of the rover's arm (Figure 1a). PADS produces powdered drill cuttings for analysis by the SAM (Sample Analysis at Mars) and CheMin (Chemistry and Mineralogy) instruments (Figure 1b) (Mahaffy et al., 2012 and Blake et al., 2012). PADS utilizes a 5/8 inch (~16 mm), tungsten carbide commercial hammer-drill bit optimized for percussive drilling. The chisel face, where the bit interfaces the rock, remains unmodified (Anderson et al., 2012). Under normal use, preload on the bit is maintained by the Drill Translation Mechanism, which pushes the drill bit into the rock independently of the stabilizers allowing the robotic arm to remain fixed.

Percussive energy delivered to the drill bit is provided by a voice coil mechanism that uses a magnetic field to oscillate a free mass. The free mass acts as a hammer and transfers percussion energy to the drill bit. The voice coil mechanism is decoupled from the rotary drive, adding the capability of varying the percussion energies into the rock regardless of spindle rotational velocity. Onboard software during the drilling process chooses a discrete Voice Coil Level (VCL). VCLs 1 through 6 provide single-impact

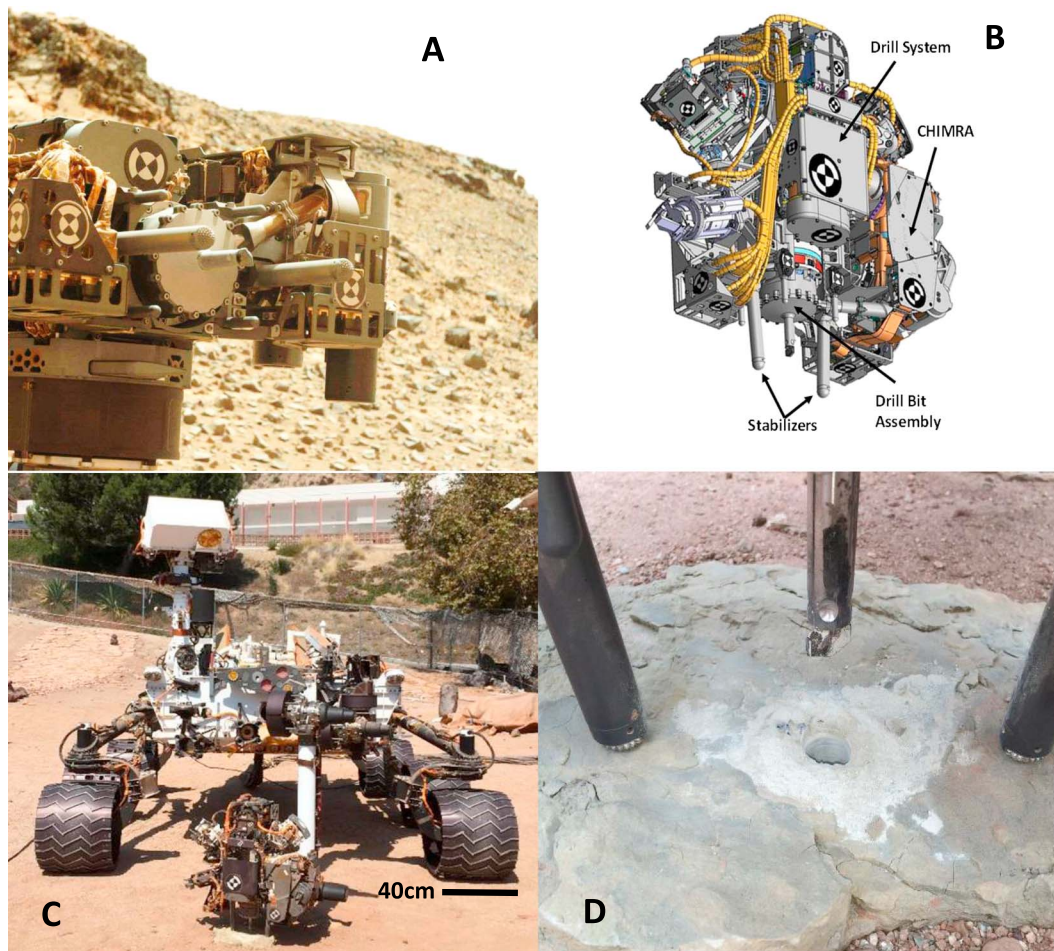


Figure 1. (a) The Powder Acquisition Drill System (PADS) imaged by Mastcam shows the rover's drill just after completion of a drilling operation at Telegraph Peak on sol 908. The drill bit assembly can be seen between the drill stabilizers (image: NASA/JPL-Caltech/MSSS). (b) Diagram of the Mars Science Laboratory (MSL) Powder Acquisition Drill System (PADS) and the Collection and Handling for In-situ Martian Rock Analysis (CHIMRA) subsystem, where the sample is sieved and portioned into a predetermined aliquot before delivery to SAM and/or CheMin (image: NASA/JPL-Caltech). (c) Vehicle System Test Bed (VSTB) in the Mars Yard at Jet Propulsion Laboratory drilling into Ridge Basin Mudstone A. (d) Close-up of the VSTB drill bit and stabilizers shortly after drilling 16 mm diameter hole into the Ridge Basin Mudstone A (image: NASA/JPL-Caltech).

energies ranging from 0.05 to 0.8 J (VCL 1 = 0.05 J, VCL 2 = 0.20 J, VCL 3 = 0.31 J, VCL 4 = 0.45 J, VCL 5 = 0.61 J, and VCL 6 = 0.80 J). The percussion rate remains 30.1 Hz regardless of VCL. In order to allow autonomous drilling, the system automatically adjusts the percussion level to maintain the prescribed rate of penetration (ROP) and weight on bit (WOB) between parameterized thresholds. The percussion level, determined prior to launch, has been held to a maximum of VCL-4 for all MSL drill campaigns to date.

The MSL Mission has employed two sets of control algorithms for drilling operations. The first four drilling campaigns at outcrops John Klein on Sol 182, Cumberland on Sol 279, Windjana on Sol 621, and Confidence Hills on Sol 759 were conducted using a drilling configuration designed prior to launch that minimizes the total drilling duration by biasing toward the *highest* VCL necessary to make progress into the sample (Helmick et al., 2013). This original operational profile, called the standard percussion algorithm, worked to maintain between 50 and 80 N of force on the bit and started at the highest allowable percussion energy at VCL-4. The percussion energy was stepped down to lower VCLs if the drill could not maintain WOB greater than 50 N. The ROP is limited to a maximum of 0.25 mm/s during normal drilling operations. An inability to maintain WOB above 50 N at the maximum ROP indicates that the rock is being fractured too aggressively. If the system fell below 0.16 mm/s ROP, the percussion energy was stepped back up successively to increase ROP to the prescribed rate.

Starting the drilling operation at the highest allowable percussion level created some problems under certain conditions. Rocks that were poorly embedded or too weak moved or fractured under the initial higher percussion levels. Following an abandoned drill opportunity at the Bonanza King target on Sol 724, when the rock moved under percussion of a presampling operation (minidrill), the engineering team worked to develop a second, more adaptive “reduced percussion” configuration. Weeks of testing in terrestrial rocks resulted in the development of the reduced percussion algorithm, which monitors ROP and WOB thresholds, guiding the VCL control algorithm toward the *lowest* VCL possible while still maintaining adequate ROP into the rock. Reduced percussion initiates the drill operation sequence at the lowest percussion level of VCL-1 and only increases percussive energy when the ROP falls below 0.05 mm/s. The system will continue to increase VCL up to a maximum of VCL 4 and will eventually stop the drilling process (i.e., fault out) if the ROP falls below 0.025 mm/s while at VCL-4.

After a minidrill attempt on Sol 867 at the Mojave target resulted in a fractured slab, the decision was made to put the reduced percussion algorithm into service. During the next drill attempt, on Sol 882, reduced percussion was successfully used to sample the Mojave 2 target. Since then, reduced percussion has been used to drill 10 additional rocks. The last full depth drilling operation that used the reduced percussion algorithm took place on Sol 1462 at the Quela outcrop.

The drilling performance in the 11 rocks drilled using reduced percussion is used herein to indicate the strengths of the rocks at Gale. Reduced percussion presented a major advantage to this investigation. In the first four drill campaigns, John Klein, Cumberland, Windjana, and Confidence Hills, standard percussion may have allowed significant portions of the rocks to be drilled at higher percussive energies than needed. Knowing how much energy is delivered, even when rock fails under the bit, is not the same as knowing how much energy was needed to fail the rock. During reduced percussion, the drill begins at the lowest percussion energy and then reacts to stronger rocks by incrementally increasing VCL until the rocks begins to fail under the bit at the prescribed ROP. Similarly, to determine the strengths of rocks, geotechnical instruments deliver increasing force in a systematic manner (Bieniawski & Bernede, 1979). For instance, the pressure at which the rock fails in compression determines the compressive strength of a rock. If more force than necessary were immediately delivered, one would only know that the strength of the rock had been exceeded. Yet, rock strength would not be quantifiable. A systematic lead-up to failure is essential for both typical rock strength measurements in the laboratory and when using drill performance as an indicator of rock strength.

During reduced percussion, the drill ultimately reaches a VCL that maintains the prescribed ROP. As the percussive energy is systematically increased, where rocks are composed of equitable sedimentary assemblage, one can know if one rock on Mars is stronger than another just by knowing that it had necessitated a higher VCL to maintain the prescribed ROP. Of course, with only four VCLs available, there is little resolution. There have been multiple rocks that have caused the system to fall within the prescribed ROP at the same percussion level. Therefore, the specific percussion energy necessitated by each rock at the highest VCL achieved is calculated and used to indicate rock strength. Rocks requiring more percussive energy at the highest VCL achieved are stronger than those requiring less percussive energy within the respective - highest-VCL-achieved.

In order to normalize the data, the energy (J) is calculated over the volume (cm^3) of rock comminuted during the generation of the borehole. Prior to reaching the VCL that maintains the prescribed ROP, the system works at lower VCLs; percussive energy is expended, but there is little to no progress into the rock. Therefore, no significant volume is excavated from the borehole, resulting in disproportionately high energies per unit volume.

Drill performance herein is reported for full-depth drilling operations only. Prior to drilling, a hole-start operation is performed. During “hole start,” a divot of 5 mm depth is created. This safeguards concentricity to the projected hole by ensuring that the tapered end of the bit is fully engaged into the rock. As such, the cross section of the drill bit remains constant as does the volume-per-unit-depth excavated throughout the drilling operation post hole start.

During drilling operation, as the system works to maintain the WOB, the time spent at each VCL is known, as is the ROP and the depth drilled. The diameter of the bit remains constant, so as bore depth is achieved, the volume of rock that was processed under the bit is calculated at 0.18 cm^3 of rock excavated per millimeter

of depth drilled. The specific percussive energy (E_{Percus}) can be calculated from the time (t) in seconds, the energy per blow of the VCL (E_{VCL}), and the rate of percussion (30.1 Hz) over the volume of material (vol) removed using:

$$E_{\text{Percus}} = \frac{30.1 \cdot t \cdot E_{\text{VCL total}}}{\text{vol}} \quad (1)$$

At the time of this writing, 11 outcrops on Mars have been drilled using the reduced percussion algorithm. Seven of these sites represent Murray formation outcrops, with four representing the Stimson formation. The Murray formation is composed of mudstones, interpreted as lacustrine, characterized by fine-scale planar laminations and grains sizes that range from very fine sand to coarse silt, with Krumbein values of $3(\phi)$ (125 μm) to $5(\phi)$ (300 μm) (Sloss, 1963) (Sacks et al., 2016). The Stimson formation is an eolian sandstone interpreted as dune formation. Stimson outcrops are found locally and unconformably atop of the Murray. The Stimson formation is dominated by very fine sand grains, $1(\phi)$ (0.5 mm) to $4(\phi)$ (63 μm). The Stimson and Murray rocks are lithified fine sandstones and coarse silty mudstones, respectively, with varying compressive strengths. Thomson et al. (2013, 2014) illustrated that the energy per unit volume needed to break the bonds of a volume of rock correlates to uniaxial compressive strength (UCS).

Even with a chisel style drill bit optimized for percussion, it is understood that rotation contributes to comminution, especially in weaker rocks. Yet specific percussion energy, as opposed to total drill energy, was used to calculate rock strengths herein. Indentation into the surfaces of rocks under a load is the origin of all rock comminution processes (Teale, 1965). In the case for PADS, the dominant factor for rock comminution is high-impact velocity focused along the edge of the drill bit that produces concentrated forces pulverizing the rock in a zone extending several times greater than the depth of the indentation (Han et al., 2005).

During this research, rocks were drilled at Earth ambient pressures for comparison to rocks drilled on Mars. Atmospheric pressure does not have a significant effect on the manner in which stresses are carried through solid materials. A rock's solid components will react the same to percussive energy regardless of the background atmospheric pressure. This does not hold true for the rotary drill component. During testing with drills optimized for rotary drilling, friction between rock surfaces and drill bits have been found to be as much as 10% lower at Mars atmospheric pressure than at Earth ambient pressure (Zacny & Cooper, 2007). This is likely due to desorption of gas molecules from surfaces allowing for less rotational torque. This effect may also provide for more efficient cuttings removal in the presence of a percussive element at lower pressures (Green & Zacny, 2014).

2. Materials and Methods

Terrestrial, sedimentary rocks from the Ridge Basin Group in California were drilled at Earth ambient pressure using the arm-mounted drill on the Vehicle System Test Bed (VSTB) in the Mars Yard at the Jet Propulsion Laboratory (JPL) (Figures 1c and 1d). This was done to provide a direct comparison of the drill performances measured during the mission. The VSTB's robotic arm and drill system are mechanically indistinguishable from the drill system and robotic arm aboard the Curiosity rover (Robinson et al., 2013).

The Ridge Basin rocks were selected as Gale crater analogs based on their sedimentary history and morphological characteristic, which are reasonable comparisons to the Martian rocks encountered by Curiosity to date. Similar to the sedimentary environment at Gale crater, the siltstones and sandstones of the Ridge Basin Group were produced as a result of high-relief infilling into a restricted basin (Link & Osborne, 2009). Conglomerates, fine sandstones, and silty mudstones at both sites provide evidence of energetic fluvial activity into mudflats, shallows, and near-offshore beds. Ridge Basin sandstones are likely of marginal shoreline origin, whereas the fine sandstones of the Stimson formation at Gale Crater are thought to have been deposited in an eolian dune system (Banham et al., 2017). Where the clastic components of all of the sedimentary rocks encountered at Gale crater have been dominantly basaltic in composition, Ridge Basin rocks are composed of a variety of felsic to arkosic clastic components. Clasts of Ridge Basin conglomerates are largely granitic in composition. Sandstones are mainly lithic plagioclase arkoses containing small amounts of carbonate constituents. Illite and smectite with minor kaolinite comprise the detrital clays found in the Ridge Basin

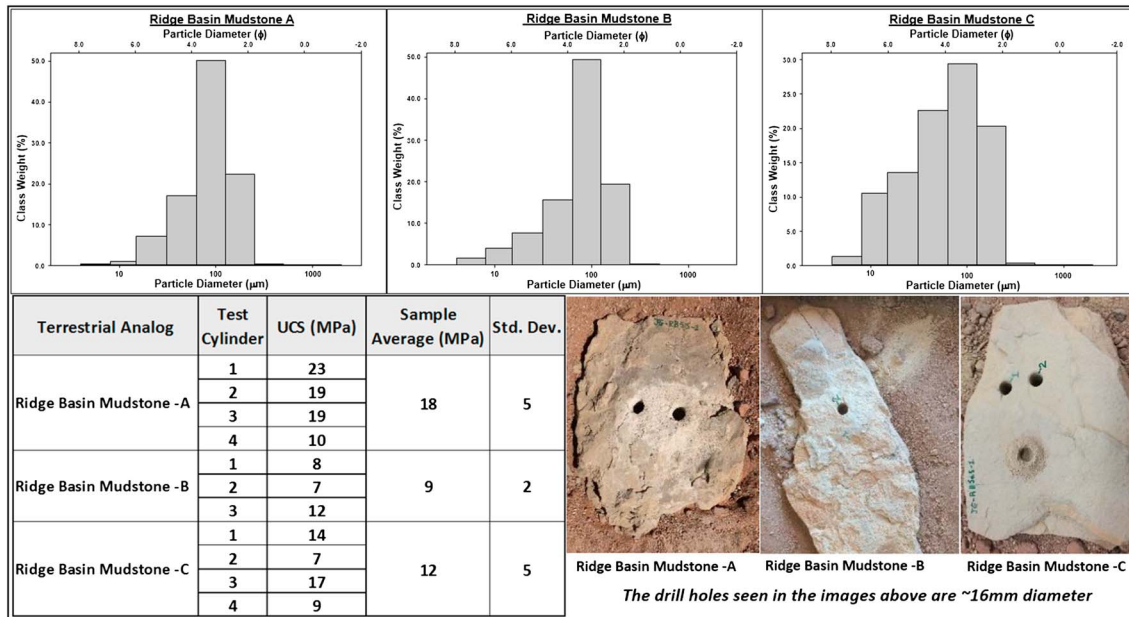


Figure 2. Summary of the measured properties of the Ridge Basin mudstones that were used as terrestrial analogs for the Murray and Stimson on Mars. Grain size distribution analysis illustrates that the Ridge Basin rocks are fine-grained mudstones. Results of the uniaxial compressive strength testing are illustrated on the bottom left, and images of each of the samples drilled during this research are illustrated on the bottom right (image: NASA/JPL-Caltech).

Siltstones (Link, 1984), while the clastic components of the fine-grained sediments of Ridge Basin are generally arkosic, and the clastic grains at Gale are generally basaltic. However, the mineralogy of the grains themselves is not relevant for comparing rock strength in this case. Both arkosic and basaltic grains are of equitable hardness of 6–7 on the Mohs scale (Pough, 1996).

Rocks collected from the Ridge Basin group include three specimens of varied UCS (Figure 2). Particle size distribution for each was determined by wet sieving disaggregated samples. Following disaggregation, each specimen was wet-sieved using a 0.0625 mm mesh in order to separate the sand and mud fractions in each. After drying, the sand fraction was sieved for 15 min. The mud fraction in each specimen was analyzed via pipette analysis (Folk, 1980). All three Ridge Basin samples can be classified as moderately sorted, muddy sandstones dominated by fine, very-fine-sand-sized and very-coarse-silt-sized grains (Figure 2). Mean grain sizes were found to be 82 μm (Phi value of 3.6 φ) for Ridge Basin Mudstone A, 74 μm (Phi value of 3.8 φ) for Ridge Basin Mudstone B, and 56 μm (Phi value of 4.1 φ) for the Ridge Basin Mudstone C.

One of the factors that affects drill performance is the ratio of grain size to drill bit diameter. Boring into a conglomerate will affect drilling performance more profoundly than would a homogenous sandstone, even where lithification mineralogy and maturity remained equal. However, the grain sizes of the Murray, Stimson, and the Ridge Basin mudstones are small relative to the drill bit diameter (0.003 mm:16 mm). The largest difference in the mean particle sizes among the Murray, Stimson, and Ridge Basin mudstones is ~300 μm, which is ~53 times smaller than the diameter of the drill bit. With such a small difference in grain sizes among these siltstones and sandstones, and such a large bit-diameter to grain size ratio, the difference in sedimentary classification among the rocks does not affect the drill performance significantly. As such, the specific percussion energy per unit excavated and the rock strengths for all formations under investigation have been evaluated together.

The unconfined compressive strengths of each of the three Ridge Basin samples were determined according to ASTM D7012C on multiple cored samples to ensure a representative distribution of the parent rock (Figure 2). One inch diameter cores were taken using a wet coring system. However, dry nitrogen replaced water as a working fluid to ensure no adsorbed water infusion into the test articles, which could have weakened them. The cores were cut to 2 inch length cylinders. UCS testing on the cylinders created from the cores was conducted at ambient atmospheric conditions.

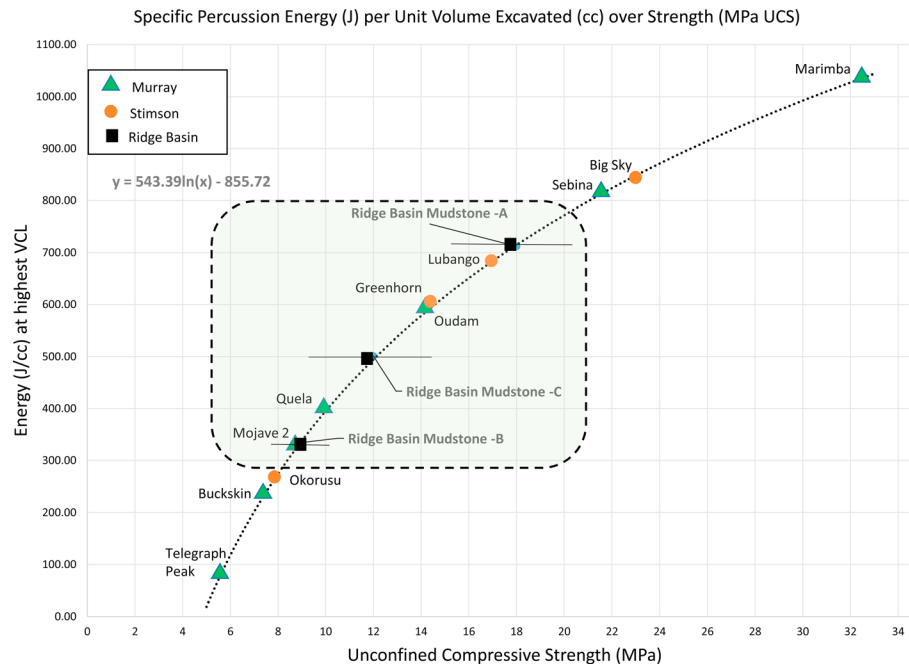


Figure 3. Illustration of the specific percussion energy per unit volume excavated at the highest VCL versus the rock strength (UCS). Rocks presented here are those that have been drilled using the reduced percussion algorithm during the MSL mission (Murray and Stimson) and rocks that have been drilled using the reduced percussion algorithm with the Vehicle System Test Bed (VSTB) at JPL (Ridge Basin). A strength curve was generated by plotting the percussion energies needed to drill into the three Ridge Basin rocks over their (known) UCS. The percussive energy per unit volume excavated measured for each rock drilled at Gale is plotted along the strength curve to indicate plausible UCS for each. Error reported for the Ridge Basin mudstones is represented as the standard deviation in strength during UCS testing. The authors are confident in the strengths reported within the green highlighted area.

3. Results and Discussion

Each of the Ridge Basin rocks were drilled once using the VSTB with the reduced percussion algorithm precisely as they would have been drilled on Mars. Percussion energy per unit volume excavated was calculated using equation (1). The specific percussion energy per volume excavated and the strengths of the Ridge Basin mudstones can be found in Figure 3 and in Table 1.

The specific percussion energy needed to drill the 11 rocks at Gale are plotted along a strength curve as shown in Figure 3. Here is a word of caution when interpreting Figure 3. The curve, defined by the equation in the figure, is determined using only three points that define the calibration range. This calibration range is determined by the testing in the Ridge Basin mudstones of which we know the strengths and the energies needed to drill (black squares in Figure 3). The area outside the green shaded calibration zone represents an extrapolation that assumes similar lithologies. Error reported for the Ridge Basin mudstones is represented as the standard deviation in strength during UCS testing (Figure 3).

Sedimentary classification plays an important role in a sedimentary rock's ability to resist drilling. Particle size distribution, shape, and compaction determine porosity in the absence of a cementing mineral. Cementation is influential in contributing to the strength of sedimentary rocks as the type of cementing minerals determine the strength of the cement itself, and lithification-maturity determines the concentration in which the cement occupies pore spaces. The predominant cementing agent on Earth consists of very strong syntaxial quartz overgrowths. As such, sandstones and siltstones in excess of 180 MPa UCS are common on Earth (McBride, 1989). Even a relatively highly porous quartz-bound sandstone will be stronger than a fully indurated sulfate-bound sandstone (Bernabé et al., 1992). Where cement mineralogy remains constant, porosity has the greatest effect on the strength (Carey et al., 2017; Consoli et al., 2011). The sedimentary composition at Gale crater is basaltic; concentrations of silica available for quartz induration and the necessary aqueous processes are considerably less active when compared to Earth.

Conclusive evidence linking mineralogy to the rock strength at Gale remains elusive. Mineral comparisons in the Murray seem to suggest that where crystalline SiO_2 content is high, rocks tend to be weaker. This seems

Table 1
Drill Data Collected for Several Drilling Operations at Both the Murray and Stimson Sites on Mars, as Well as Ridge Basin Mudstones

Rock name	Sol	VCL 1			VCL 2			VCL 3			VCL 4			UCS (MPa)
		Time (s)	Depth (mm)	Energy (J/cm ³)	Time (s)	Depth (mm)	Energy (J/cm ³)	Time (s)	Depth (mm)	Energy (J/cm ³)	Time (s)	Depth (mm)	Energy (J/cm ³)	
Murray				90.06										
Telegraph Peak	908	610	56.63											< 8
Buckskin	1060	340	24.07	118.13	230	30.18	254.91							< 8
Mojave 2	882	290	29.72	81.59	270	26.92	335.49							~ 8.5
Quela	1464	150	18.61	67.39	220	14.29	515.07	180	23.12	403.57				8.5-12
Oudam	1361	10	0.68	122.96	120	10.07	398.62	540	47.09	594.41				12-18
Sebina	1495	190	22.71	69.96	10	1.19	280.81	290	21.27	706.82	150	13.63		> 18
Marimba	1422	330	30.37	90.85	20	3.81	175.42	70	3.11	1166.79	300	21.64		> 18
Stimson				275.94										< 8.5
Okorusu	1332	420	36.53	96.14	180	21.82								
Greenhorn	1137	10	0.01	0.00	40	2.31	579.12	190	18.64	528.49	310	38.35		12-18
Lubango	1320	10	0.00	0.00	20	1.35	496.58	240	18.37	677.19	350	38.53		12-18
Big Sky	1119	10	0.98	85.23	70	3.82	613.66	100	8.03	645.48	500	44.08		> 18
Ridge Basin				334.44										8-10
Mudstone - B		170	16.00	88.84	410	41.00								
Mudstone - C		140	19.00	61.61	450	37.00	406.76	50	4.00	647.99	40	6.00		9-15
Mudstone - A		20	0.00	0.00	10	0.00	0.00	10	0.00	0.00	530	56.00		16-21

Note. Several drilling operations did not reach higher VCLs, as shown by the gray boxes. The specific percussion energy delivered at the highest VCL achieved at each site is highlighted in green.

to hold true, to a lesser extent, in samples composed of relatively high percentages of magnetite. It may be that crystalline SiO_2 and magnetite are present as nonbinding, clastic components, while hematite and calcium sulfate provide the most effective chemically derived cementing mineral. It is also thought that an effective detrital cement is present in the form of phyllosilicate (clays). Under the dry conditions on the surface of Mars, these clays are likely to have solidified into an effective cement.

The outcrop at Telegraph Peak is dominated by crystalline SiO_2 and magnetite but is composed of very little hematite and virtually no calcium sulfate or phyllosilicates (Rampe et al., 2017). As such, Telegraph Peak remains the weakest rock drilled at Gale to date. Similarly, Buckskin, the second weakest rock, is also composed of a high percentage of crystalline SiO_2 , no phyllosilicates or hematite, and only a small percentage of calcium sulfate. The strongest rocks of the Murray were found to be the outcrops at Sebina and Marimba, each with a very high percentage (~40%) of phyllosilicate (Rampe et al., 2017). The first attempt to drill at the Marimba outcrop failed due to low ROP. The second attempt at Marimba, using the same reduced percussion algorithm, was successful but required $1,043 \text{ J/cm}^3$ specific percussion energy to drill to full depth. This suggests that high percentages of phyllosilicates produce higher strengths. However, the outcrop at Quela is a close mineralogical match to Sebina and Marimba yet remains noticeably weaker. Oudam, with very little phyllosilicate, is stronger than Quela, although the largest mineral component within Oudam is hematite. This high percentage of hematite may account for the additional strength of the outcrop at Oudam in the absence of a phyllosilicate cement.

Decisive trends linking rock strength to mineralogy are even more elusive in the Stimson outcrops. The weakest Stimson outcrop at Okousu and the strongest outcrop at Big Sky are mineralogically very similar. The only discernable difference among these two outcrops is that the magnetite concentration within Okoruso is markedly higher and the hematite percentage was found to be lower than in Big Sky. This would suggest that hematite is the primary cementing mineral in the Stimson formation. However, the outcrop at Greenhorn holds the highest percentage of hematite of all Stimson outcrops tested yet remains in family concerning strength among other Stimson rocks (Treiman et al., 2016). As such, it is evident that factors other than mineral abundances are playing a role in the rock strength story at Gale crater.

It is believed that the crater has been the site of water table undulations, each bringing mineral cements that have permeated the formation. Gale has also been subjected to multiple burial events (Yen et al., 2017). The Stimson is a product of one of these burial events as evidenced by its unconformable contact atop of the Murray. While the Stimson and Murray are both lithified with secondary minerals, the Murray is lower in the formation and has been subjected to higher burial pressures and more fluid infiltration events. Weaker rocks of both formations may be the result of mineral depletion as fluids have moved through them creating open pore-spaces.

While both Stimson and Murray rocks remain within a reasonable strength range for calcium sulfate and hematite bound rocks, they present the weakest end when compared to terrestrial analogs. Hematite and gypsum bound rocks are generally stronger than 20 MPa and are known to reach strengths up to 40 MPa (Yilmaz & Sendir, 2002). It is possible that the rocks drilled at Gale have never been fully indurated with cementing minerals. The time during which these rocks were subjected to fluids bringing fortifying minerals may have been inadequate to provide full induration. There is also the possibility that the rocks at Gale are fully indurated and have been subjected to mineral depletion, diurnal temperature cycling, neighboring impact events, reactive phyllosilicate swell/shrink cycles, the compression of burial, and the subsequent decompression due to exhumation.

4. Conclusions

The weakest rocks at Gale are no stronger than adobe bricks (1.5–5 MPa) Silveira et al., 2012), and the strongest rocks drilled can be compared to the strength of a standard concrete sidewalk or driveway (15–30 MPa) (Teychenné et al., 1997). The Murray and Stimson are composed of relatively weak rocks when compared to quartz-indurated sandstones and siltstones found on Earth. As such, Murray and Stimson outcrops are more akin to geologically immature, terrestrial sandstones, and siltstones.

While PADS was not designed to be an instrument for measuring rock properties, the method employed has provided a good indicator of the strengths of the rocks drilled at Gale crater. These techniques and methodologies will be useful during future missions during which rotary percussive drilling will be employed.

Acknowledgments

This research was carried out at the Jet Propulsion Laboratory, California Institute of Technology, under a contract with the National Aeronautics and Space Administration. The authors acknowledge the extraordinary work executed by the MSL engineering and science operations teams. We thank Juergen Schieber, Bernard Hallet, Ronald Sletten, Kris Zacny, and Bradley Thomson whose comments and guidance have greatly improved this manuscript. Readers can access the data underlying the manuscripts conclusions in this repository: <https://issues.pan-gaea.de/browse/PDI-16486>.

References

- Anderson, R. C., Jandura, L., Okon, A. B., Sunshine, D., Roumeliotis, C., Beegle, L. W., ... Robinson, M. (2012). Collecting samples in Gale crater, Mars; an overview of the Mars Science Laboratory sample acquisition, sample processing and handling system. *Space Science Reviews*, 170(1-4), 57–75. <https://doi.org/10.1007/s11214-012-9898-9>
- Arvidson, R. E. (2016). Aqueous history of Mars as inferred from landed mission measurements of rocks, soils, and water ice. *Journal of Geophysical Research: Planets*, 121, 1602–1626. <https://doi.org/10.1002/2016JE005079>
- Banham, S. G., Gupta, S., Rubin, D. M., Watkins, J. A., Sumner, D. Y., Grotzinger, J. P., & Bell, J. F. (2017). The Stimson formation: Determining the morphology of a dry aeolian dune system and its significance in Gale crater, Mars. In Lunar and Planetary Science Conference (Vol. 48). Bernabé, Y., Fryer, D. T., & Hayes, J. A. (1992). The effect of cement on the strength of granular rocks. *Geophysical Research Letters*, 19(14), 1511–1514. <https://doi.org/10.1029/92GL01288>
- Bieniawski, Z. T., & Bernede, M. J. (1979). Suggested methods for determining the uniaxial compressive strength and deformability of rock materials: Part 1. Suggested method for determining deformability of rock materials in uniaxial compression. In *International journal of rock mechanics and mining sciences & geomechanics abstracts* (Vol. 16(2), pp. 138-140). Pergamon, England.
- Blake, D., Vaniman, D., Achilles, C., Anderson, R., Bish, D., Bristow, T., ... Downs, R. T. (2012). Characterization and calibration of the CheMin mineralogical instrument on Mars Science Laboratory. *Space Science Reviews*, 170(1-4), 341–399. <https://doi.org/10.1007/s11214-012-9905-1>
- Carey, E. M., Peters, G. H., Choukroun, M., Chu, L., Carpenter, E., Cohen, B., ... Shiraishi, L. R. (2017). Development and characteristics of mechanical porous ambient comet simulants as comet surface analogs. *Planetary and Space Science*, 147, 6–13. <https://doi.org/10.1016/j.pss.2017.08.010>
- Consoli, N. C., Dalla Rosa, A., Corte, M. B., Lopes, L. D. S. Jr., & Consoli, B. S. (2011). Porosity-cement ratio controlling strength of artificially cemented clays. *Journal of Materials in Civil Engineering*, 23(8), 1249–1254. [https://doi.org/10.1061/\(ASCE\)MT.1943-5533.0000283](https://doi.org/10.1061/(ASCE)MT.1943-5533.0000283)
- Folk, R. L. (1980). *Petrology of sedimentary rocks*. Cedar Hill, TX: Hemphill Publishing Company.
- Green, A., & Zacny, K. (2014). Effect of Mars atmospheric pressure on percussive excavation forces. *Journal of Terramechanics*, 51, 43–52. <https://doi.org/10.1016/j.jterra.2013.11.001>
- Grotzinger, J. P., et al. (2014). A habitable fluvio-lacustrine environment at Yellowknife Bay, Gale crater, Mars. *Science*, 343(6169), 1242777. <https://doi.org/10.1126/science.1242777>
- Han, G., Bruno, M., & Dusseault, M. B. (2005). Dynamically modelling rock failure in percussion drilling. In Alaska Rocks 2005, The 40th US Symposium on Rock Mechanics (USRMS). American Rock Mechanics Association.
- Helmick, D., McCloskey, S., Okon, A., Carsten, J., Kim, W., & Leger, C. (2013). Mars Science Laboratory algorithms and flight software for autonomously drilling rocks. *Journal of Field Robotics*, 30(6), 847–874. <https://doi.org/10.1002/rob.21475>
- Link, M. H. (1984). Fluvial facies of the Miocene ridge route formation, Ridge Basin, California. *Sedimentary Geology*, 38(1-4), 263–285. [https://doi.org/10.1016/0037-0738\(84\)90082-4](https://doi.org/10.1016/0037-0738(84)90082-4)
- Link, M. H., & Osborne, R. H. (2009). Lacustrine facies in the Pliocene Ridge Basin group: Ridge Basin, California. Modern and ancient lake sediments. *Special Publication*, 2, 169–187.
- Mahaffy, P. R., Webster, C. R., Cabane, M., Conrad, P. G., Coll, P., Atreya, S. K., ... Brinckerhoff, W. B. (2012). The sample analysis at Mars investigation and instrument suite. *Space Science Reviews*, 170(1-4), 401–478. <https://doi.org/10.1007/s11214-012-9879-z>
- McBride, E. F. (1989). Quartz cement in sandstones: A review. *Earth-Science Reviews*, 26(1-3), 69–112. [https://doi.org/10.1016/0012-8252\(89\)90019-6](https://doi.org/10.1016/0012-8252(89)90019-6)
- Pough, F. H. (1996). *A field guide to rocks and minerals*. Boston: Houghton Mifflin Harcourt.
- Rampe, E. B., Ming, D. W., Grotzinger, J. P., Morris, R. V., Blake, D. F., Vaniman, D. T., ... & Downs, R. T. (2017). Mineral trends in early Hesperian lacustrine mudstone at Gale crater, Mars.
- Robinson, M., Collins, C., Leger, P., Kim, W., Carsten, J., Tompkins, V., ... & Florow, B. (2013). Test and validation of the Mars Science Laboratory robotic arm. In System of Systems Engineering (SoSE), 2013 8th International Conference on (pp. 184–189). IEEE.
- Sacks, L. E., Edgar, L. A., Edwards, C. S., & Anderson, R. B. (2016). Grain-scale analyses of Curiosity data at Marias Pass, Gale crater, Mars: Methods comparison and depositional interpretation. In AGU Fall Meeting Abstracts.
- Silveira, D., Varum, H., Costa, A., Martins, T., Pereira, H., & Almeida, J. (2012). Mechanical properties of adobe bricks in ancient constructions. *Construction and Building Materials*, 28(1), 36–44. <https://doi.org/10.1016/j.conbuildmat.2011.08.046>
- Sloss, L. L. (1963). *Stratigraphy and sedimentation*. San Francisco: WH Freeman.
- Teale, R. (1965). The concept of specific energy in rock drilling. In *International journal of rock mechanics and mining sciences & geomechanics abstracts* (Vol. 2(1), pp. 57-73). Pergamon, Turkey: Pergamon.
- Teychenné, D. C., Franklin, R. E., Erntroy, H. C., Nicholls, J. C., Hobbs, D. W., & Marsh, D. (1997). Design of normal concrete mixes.
- Thomson, B. J., Bridges, N. T., Cohen, J., Hurowitz, J. A., Lennon, A., Paulsen, G., & Zacny, K. (2013). Estimating rock compressive strength from Rock Abrasion Tool (RAT) grinds. *Journal of Geophysical Research: Planets*, 118, 1233–1244. <https://doi.org/10.1002/jgre.20061>
- Thomson, B. J., Hurowitz, J. A., Baker, L. L., Bridges, N. T., Lennon, A. M., Paulsen, G., & Zacny, K. (2014). The effects of weathering on the strength and chemistry of Columbia River basalts and their implications for Mars exploration rover Rock Abrasion Tool (RAT) results. *Earth and Planetary Science Letters*, 400, 130–144. <https://doi.org/10.1016/j.epsl.2014.05.012>
- Treiman, A. H., Bish, D. L., Vaniman, D. T., Chipera, S. J., Blake, D. F., Ming, D. W., ... Rampe, E. B. (2016). Mineralogy, provenance, and diagenesis of a potassic basaltic sandstone on Mars: CheMin X-ray diffraction of the Windjana sample (Kimberley area, Gale crater). *Journal of Geophysical Research: Planets*, 121, 75–106. <https://doi.org/10.1002/2015JE004932>
- Yen, A. S., Ming, D. W., Vaniman, D. T., Gellert, R., Blake, D. F., Morris, R. V., ... Treiman, A. H. (2017). Multiple stages of aqueous alteration along fractures in mudstone and sandstone strata in Gale crater, Mars. *Earth and Planetary Science Letters*, 471, 186–198. <https://doi.org/10.1016/j.epsl.2017.04.033>
- Yilmaz, I., & Sendir, H. (2002). Correlation of Schmidt hardness with unconfined compressive strength and Young's modulus in gypsum from Sivas (Turkey). *Engineering Geology*, 66(3-4), 211–219. [https://doi.org/10.1016/S0013-7952\(02\)00041-8](https://doi.org/10.1016/S0013-7952(02)00041-8)
- Zacny, K. A., & Cooper, G. A. (2007). Friction of drill bits under Martian pressure. *Journal of Geophysical Research*, 112, E03003. <https://doi.org/10.1029/2005JE002538>